Photon production in an expanding and chemically equilibrating gluon-enriched plasma

B. KÄMPFER[a,b], O.P. PAVLENKO[a,c]

[a]Research Center Rossendorf, Institute for Nuclear and Hadron Physics
PF 510119, 01314 Dresden, Germany
[b]Inst. Theor. Phys. (KAI e.V.), TU Dresden, Germany
[c]Institute for Theoretical Physics, Kiev, Ukraine

Abstract

Photon production in a longitudinally and transversely expanding gluon plasma with initially little quark admixture is considered. Chemical equilibration of quarks and gluons is followed by rate equations. The yields of hard photons with $E \geq 2$ GeV are insensitive to chemical equilibration and depend mainly on the initial thermalized state. Medium-energy photons with $E \sim 1$ GeV are more frequently produced in case of faster equilibration, despite of faster cooling. For an assumed fast equilibration we follow the evolution of matter through mixed and hadron phases. The transverse momentum kick, due to transverse expansion, of photons from hadron matter is shown to be reduced for an equation of state with reduced latent heat. The photon yield in the region $E > 1$ GeV from deconfined matter dominates for conditions, estimated to be achieved at RHIC, in case of a weakly first-order confinement transition.

1 Introduction

Future ultra-relativistic heavy-ion experiments, such as the lead beam project at CERN-SPS, or the RHIC project, or the LHC plan, are aimed to search for deconfinement effects in dense and hot nuclear matter. In the very first reaction stage of the colliding nuclei there are hard parton scatterings which produce a part of secondaries, e.g., in mini-jets [1]. Due to semi-hard interactions the partons evolve towards local equilibrium, however, in strong competition with the rapid (mainly longitudinal) expansion of the matter. Hard and semi-hard scatterings in parton matter can be calculated within the framework of perturbative QCD. Perturbative cross sections for gluon-gluon interaction are larger than the ones for quark-quark or quark-gluon scatterings. This fact seems to imply that in ultra-relativistic heavy-ion collisions probably a gluon plasma is initially created with only a few quarks admixed [2, 3]. Present parton cascade models support such a picture [4, 5, 6, 7, 8]. The large gluon-gluon cross section helps to thermalize quickly the gluon system. In a second reaction stage the few quarks and the gluons thermalize. Even being early in thermal equilibrium such a gluon plasma with quark admixture is still in a chemical off-equilibrium state for some time. On a larger time scale the chemical equilibration proceeds. Also the gluon phase space might be undersaturated, and gluon multiplication till saturation needs some time. Since many of the proposed probes of the quark-gluon plasma rely on indirect measurements of the deconfined quark matter distribution it seems to be necessary to refine the standard estimates which assume chemical equilibrium. The present lattice QCD calculations [9] are addressed to equilibrium (thermal, chemical and mechanical) properties of a quark-gluon plasma or a pure gluon plasma [10].

The aim of our paper is to analyze the thermal photon production (cf. [11] and Refs. quoted therein) in an expanding gluon plasma, which is initially in thermal equilibrium (also with the quark admixture), and which equilibrates towards chemical equilibrium by quark and gluon production. Various aspects of the equilibration are dealt with rate equations [8, 12] or within the parton cascade model [6]. We investigate here how the chemical equilibration process can affect the photon yields. Since we employ a complete model, which includes longitudinal and transverse expansion till freeze-out, we can follow the evolution of equilibrated matter through a mixed phase into hadron matter. Therefore, the relation of thermal photons from deconfined matter to such ones from hadron can be quantified.

The NA34 and WA80 photon measurements at previous SPS oxygen and sulphur runs indicate that the photon spectra are dominated by hadronic decays [13]. But experimental refinements probably will allow for an identification of thermal photons.

Our paper is organized as follows. In section 2 we consider the chemical quark and gluon equilibration processes by using rate equations solved together with boost invariant scaling hydrodynamics and transverse expansion. The latter one is treated within a new global hydrodynamical scheme (presented in detail in Appendix). We use the results in section 3 to analyze the photon yield from the equilibrating plasma. While the quark-gluon phase space saturation achieved depends strongly on the reaction cross sections, we find that the photon yield is not very sensitive to the details of the chemical equilibration processes. The summary can be found in section 4. Besides the global hydrodynamics for the transverse expansion we discuss in the Appendix also the transverse momentum kick which the photons experience from the later hadronic stage. We show that for small latent heat in the confinement transition the transverse expansion is reduced (compared to the standard bag model equation of state) and the transverse momentum kick of the

photons is not strong. Hence the photon yield from the chemical off-equilibrium gluon-enriched plasma is expected dominate over the yield from hadron matter in case of a weakly first-order confinement transition.

2 Chemical evolution of quark-gluon degrees of freedom

We employ a transport model of coupled Boltzmann type equations for the parton distribution functions $f_a(p,x)$ (the subscript $a = g, q, \bar{q}$ denotes the parton species)

$$p^\mu \partial_\mu f_a(p_1,x) = \sum_k C_a^{(k)}(p_1,x), \tag{1}$$

where $\sum_k$ includes all collision types which change f_a. For instance, for the lowest order binary $2 \leftrightarrow 2$ processes $ab \leftrightarrow cd$ and ternary $2 \leftrightarrow 3$ processes $ab \leftrightarrow cde$ the Lorentz invariant collisional integrals read

$$\sum_k C_a^{(k)}(p_1,x) = \sum_{b,c,d} \mathcal{I}_{abcd}(p_1,x) + \sum_{b,c,d,e} \mathcal{G}_{abcde}(p_1,x), \tag{2}$$

$$\begin{aligned} \mathcal{I}_{abcd}(p_1,x) &= -\frac{1}{2(1+\delta_{ab})} \int d\Gamma_2 d\Gamma_3 d\Gamma_4 [f_a f_b - f_c f_d] \times \\ &\quad (2\pi)^4 \delta^{(4)}(p_1+p_2-p_3-p_4) \sum |\mathcal{M}_{2\to 2}|^2, \end{aligned} \tag{3}$$

$$\begin{aligned} \mathcal{G}_{abcde} &= -\frac{1}{2(1+\delta_{ab})} \int d\Gamma_2 d\Gamma_3 d\Gamma_4 \Gamma_5 [f_a(p_1) f_b(p_2) - f_c(p_3) f_d(p_4) f_e(p_5)] \times \\ &\quad (2\pi)^4 \delta^{(4)}(p_1+p_2-p_3-p_4-p_5) \sum |\mathcal{M}_{2\to 3}|^2. \end{aligned} \tag{4}$$

Here $p = (E, \vec{p})$ is the parton's four momentum, $x = (t, \vec{r})$ is the space-time, $d\Gamma = d^3\vec{p}/(2\pi)^3 2E$ denotes the momentum space volume element, and $\sum |\mathcal{M}|^2$ stands for the lowest order α_s squared matrix elements which are summed over spin and color and which contain the symmetrization factors of outgoing identical particles (we use units with $\hbar = c = 1$). The distribution is normalized by the parton density $g_a \int d^3\vec{p}(2\pi)^{-3} f_a(p,x) = n_a(x)$, where g_a denotes the degeneracy factor. δ_{ab} are Kronecker symbols which are introduced to avoid double countering in the entrance channel. The expression (2) might be improved by taking into account higher order perturbative corrections [12] and also non-perturbative soft parton reactions [14].

Integrating eq. (1) with (2) over $g_a \int d^3p_1 (2\pi)^{-3}$, one gets in Boltzmann approximation the evolution equations for the densities of the type (cf. [8] for a heuristic deduction)

$$\partial_\mu (n_g u^\mu) = -\sigma^{(2)} n_g^2 \left(1 - \frac{n_q}{n_q^{eq}} \frac{n_{\bar{q}}}{n_{\bar{q}}^{eq}} \left\{\frac{n_g^{eq}}{n_g}\right\}^2\right) + \frac{1}{2}\sigma^{(3)} n_g^2 \left(1 - \frac{n_g}{n_g^{eq}}\right), \tag{5}$$

$$\partial_\mu (n_q u^\mu) = \frac{1}{2}\sigma^{(2)} n_g^2 \left(1 - \frac{n_q}{n_q^{eq}} \frac{n_{\bar{q}}}{n_{\bar{q}}^{eq}} \left\{\frac{n_g^{eq}}{n_g}\right\}^2\right). \tag{6}$$

We assume isospin symmetry and charge symmetry, i.e. $n_q = n_{\bar{q}} = \frac{1}{2} n_Q$ and the density and medium four velocity are defined via the moment of the distribution function,

$n_a u^\mu = g_a(2\pi)^{-3}\int d^3pE^{-1}p^\mu f(p,x)$, where u^μ is the flow velocity. The reference equilibrium density n^{eq} is correspondingly defined by the same integral but with f_{eq}. Instead of the ratio $n_{Q,g}/n^{eq}_{Q,g}$ one can use the fugacities $\lambda_{Q,g}$ (see below). $\sigma^{(2,3)}$ stand for the thermally averaged cross sections $2 \leftrightarrow 2$, $2 \leftrightarrow 3$. Ref. [8] employs for the $gg \leftrightarrow q\bar{q}$ and $gg \leftrightarrow ggg$ reactions

$$\sigma^{(2)} = \frac{\pi\alpha_s^2 N_f}{48T^2}\left(\log\frac{81}{2\pi\alpha_s\lambda_g} - \frac{7}{4}\right)^2 \Lambda_Q, \quad \sigma^{(3)} = 4.2\alpha_s^2 T\sqrt{2\lambda_g - \lambda_g^2}n_g^{-1}\Lambda_g \tag{7}$$

(N_f is the flavor number) with $\Lambda_{Q,g} = 1$, while Ref. [12] uses another $\sigma^{(3)}$ which in turn differs from that in Ref. [15]. Straightforward calculation of $\sigma^{(2)}$ from eq. (3) gives [16]

$$\sigma^{(2)} = \frac{\pi\alpha_s^2 N_f}{24m_q^2}\left(\frac{m_q}{T}\right)^5 \int_2^\infty dz z^2\tilde{\sigma}(z)K_1\left(z\frac{m_q}{T}\right), \tag{8}$$

$$\tilde{\sigma}(z) = (1 + \frac{4}{z^2} + \frac{1}{z^4})\mathrm{arth}W - \frac{1}{8}(7 - \frac{31}{z^2})W,$$

where we introduce the infra-red regularizing thermal quark mass $m_q^2 = \frac{2}{3}\pi\alpha_s T^2$ [17]. At small values of the strong coupling constant $\alpha_s \approx 0.3$ there are substantial deviations between eqs. (7) and (8) (about a factor two), which enlarge for smaller fugacities. Since the higher order processes are found to be important [12] and also non-perturbative processes might contribute, we have introduced the factors $\Lambda_{Q,g}$, which we shall vary in order to learn about their affect on observables. Hence, instead of extending eqs. (5, 6) by higher order processes, we rely on the present form and demonstrate that, despite of large variations of the $\Lambda_{Q,g}$, the corresponding photon yields suffer only minor affection. This might justify the use of the restricted eqs. (5, 6) for the present purpose.

In order to solve the coupled rate equations one needs also an evolution equation for the temperature which determines the reference equilibrium densities n^{eq}. In case of local thermalization, and boost-invariant longitudinal expansion, and global transverse expansion, the corresponding set of equations is derived in Appendix A1. Instead of using the densities or fugacities we prefer to rewrite the basis equations into the variables total parton density $n = n_g + n_Q$ and chemical saturation parameter $x = n_g/n$ (then $n_Q = (1-x)n$),

$$\dot{n} = -\frac{n}{\tau} - n\frac{<\gamma>^{\cdot}}{<\gamma>} + \frac{1}{2}\sigma^{(3)}x^2n^2(1-\lambda_g), \tag{9}$$

$$\dot{x} = -n\sigma^{(2)}[x^2 - (1-x)^2\beta] + \frac{1}{2}\sigma^{(3)}nx^2(1-x)(1-\lambda_g), \tag{10}$$

where we use eq. (A.14) for rewriting $\partial_\mu(nu^\mu)$ in eqs. (5, 6), and $\beta = 4/9$ for $N_f = 2$. $<\gamma>$ stands for the radial integral on the Lorentz factor of transverse motion (see Appendix). The fugacities are

$$\lambda_Q = \frac{(1-x)n}{T^3}\frac{\pi^2}{g_Q}, \quad \lambda_g = \frac{xn}{T^3}\frac{\pi^2}{g_g}. \tag{11}$$

In chemical equilibrium one has $x = x_{eq} \equiv 0.4$. Quark undersaturation means $x > 0.4$. Various estimates predict initially $\lambda_g < 1$ [8, 12], then the inelastic gluon channel $gg \to ggg$ slows down somewhat the quark equilibration (see last term in eq. (10)), while density dilution due to expansion is partially counteracted, as seen from eq. (9).

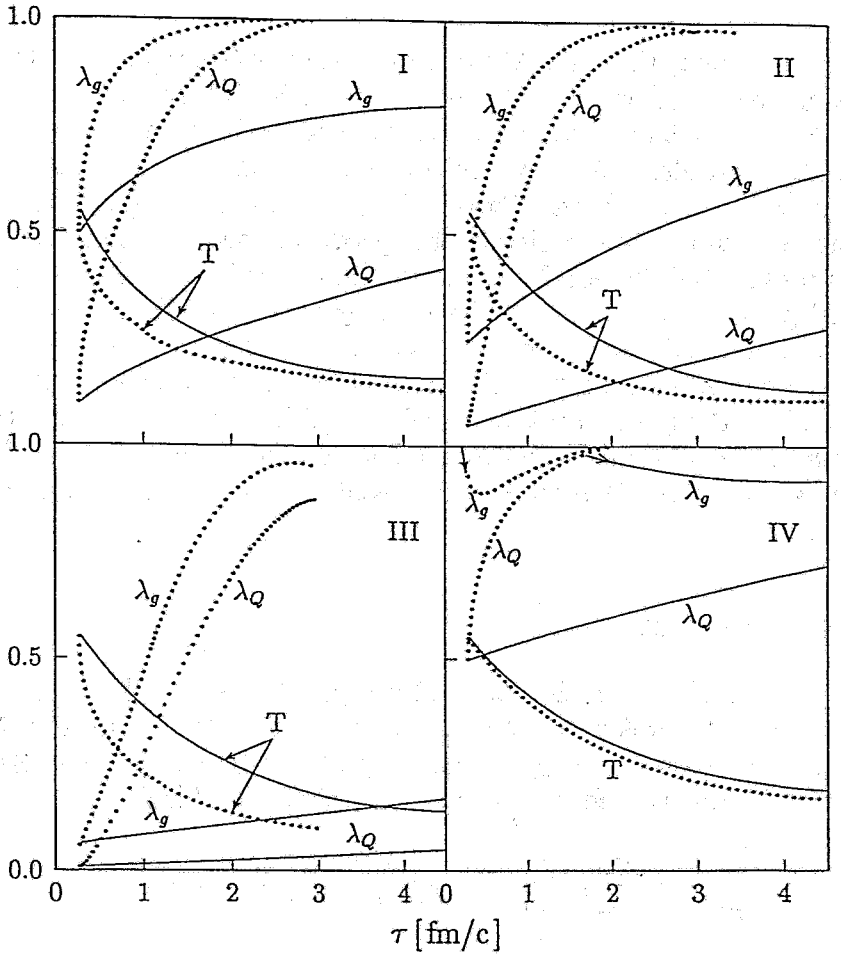

Figure 1: The time evolution of the fugacities $\lambda_{Q,G}$ and temperature T (in GeV) for the initial conditions described in text.

The inelastic reaction $gg \rightarrow ggg$ causes an increase of the comoving entropy density according to $T^3 < \gamma > \tau(\lambda_g g_g + \lambda_Q g_Q) = const$, which replaces the entropy conservation law $T^3\tau = const$ in case of pure longitudinal expansion without inelastic reactions (see Appendix, eq. (A.6)).

We study four different initial gluon fugacities. In three cases we assume $x \approx 0.8$, which corresponds to $\lambda_Q \approx \frac{1}{5}\lambda_g$, i.e., a gluon-enriched plasma with significant undersaturation of quarks. This is in line with the hot glue scenario [3] and is supported by parton cascades [5, 6, 7, 8]. The absolute fugacities differ: The predictions go from undersaturation $\lambda_g = 0.5$ (I [12]), 0.25 (II [12]), 0.06 (III [8]) to oversaturation $\lambda_g = 1.5$ (IV [6], here we use $x \approx 0.66$) for RHIC conditions. To compare not too different initial conditions, which still seem to be rather uncertain when comparing [8] and [6] as extremes, we use the unique initial time for the beginning of the thermalized era $\tau_0 = 0.31$ fm/c, and a common initial temperature $T_0 = 550$ MeV in one set of examples. In a second set we scale the initial temperature in such a way to get a constant initial energy density which corresponds to $T_0 = 550$ MeV and full equilibrations. In the latter case the initial temperatures are therefore larger than 550 MeV due to phase space undersaturation.

Solutions of eqs. (9, 10, A.12, A.13) are displayed in Fig. 1 for the first set where $T_0 = 550$ MeV. Clearly, the different initial sets show rather different time evolutions which

even more differ when varying the $\Lambda_{Q,g}$. The effect of the transverse expansion is not very important for the short-living deconfined state down to ~ 200 MeV (about 10% transverse radius increase). As expected, the faster gluon multiplication and quark pair creation are, the faster the cooling proceeds. This is particular drastic for example III. In the late stage the cooling curves are not too different. Qualitatively we recover the results of Ref. [12] for $\Lambda_g = 10$, however, due to the coupling to the quark channel and the use of different cross sections (7) we get slightly modified evolution for examples I - III. Interestingly, in case IV the initial gluon oversaturation is followed by an intermediate undersaturation because gluons are converted into $q\bar{q}$, and the backreaction $ggg \rightarrow gg$ dominates. This not included in the parton cascade [6]. The presented examples demonstrate that, in agreement with [6, 12], the gluons achieve chemical equilibrium for $\Lambda_g = 10$, while the more realistic value $\Lambda_Q \sim 1$ is insufficient to come to chemical equilibrium in the quark channel. In the extreme case III there is a competition between too fast cooling and achieving equilibrium till T_c.

3 Photon production

Now we use the above evolution of the chemical composition of the plasma to calculate the photon production. We follow the standard approaches [11] and use the dominant quark - anti-quark annihilation $q\bar{q} \rightarrow g\gamma$ and Compton like processes $gq(\bar{q}) \rightarrow q(\bar{q})\gamma$. The lowest order α_s contributions are for vanishing chemical potential [18]

$$\frac{dN_\gamma^{Comp}}{d^4x d^3p/E} = \frac{10\alpha\alpha_s}{9\pi^4} T^2 e^{-\epsilon/T} \{\log(\frac{4\epsilon T}{k_c^2}) + \frac{1}{2} - C_E\} \lambda_q \lambda_g, \tag{12}$$

$$\frac{dN_\gamma^{annih}}{d^4x d^3p/E} = \frac{10\alpha\alpha_s}{9\pi^4} T^2 e^{-\epsilon/T} \{\log(\frac{4\epsilon T}{k_c^2}) - 1 - C_E\} \lambda_q^2, \tag{13}$$

where $\epsilon = u_\mu p^\mu$, and $p^\mu = (E, \vec{p})$ denotes here the photon's four momentum, k_c is an infrared cut-off, and $C_E \approx 0.577$ stands for the Euler constant. (The effect of finite chemical potential is examined in Ref. [20]; the Landau-Pomerantschuk effect on virtual photon production is only important for soft photons [21].)

In Refs. [18, 19] the resummation technique of Braaten and Pisarski [22] has been used to regularize infra-red divergences in the rates (12, 13). Since we focus on not too soft photons with $E > T$, the photon emission turns out to depend on k_c not too sensitively. Therefore, a variant of Refs. [18, 19] with $k_c^2 = 2m_q^2 = \frac{4\pi\alpha_s}{3} T^2$ is employed.

Combining then eqs. (12, 13) one gets for the total photon rate

$$\frac{dN}{d^4x\, d^3p/E} = \frac{5\alpha\alpha_s n^2}{72^2 T^4} e^{-\epsilon/T} \{[\log(\frac{3\epsilon}{\pi\alpha_s T}) - C_E](2 - x - x^2) - \frac{1}{2}(4 - 11x + 7x^2)\}. \tag{14}$$

It can easily be seen that for $x > x_{eq} = 0.4$ the rate is suppressed in comparison with the equilibrium rate at x_{eq} [3]. This suppression depends somewhat on the photon energy and amounts roughly a factor $\frac{1}{5}$ for $x \sim 0.9$ [16]. More dramatic is the suppression of the photon yield due to overall phase space undersaturation, i.e., when n becomes smaller than the chemical equilibrium density n_{eq}. Ref. [3] claims that a higher initial temperature, compared to previous standard estimates [23], overcompensates this reduction. To be sure whether the photons an really probe the deconfined matter state we quantify below the relation of photons from deconfined matter to photons from hadron gas.

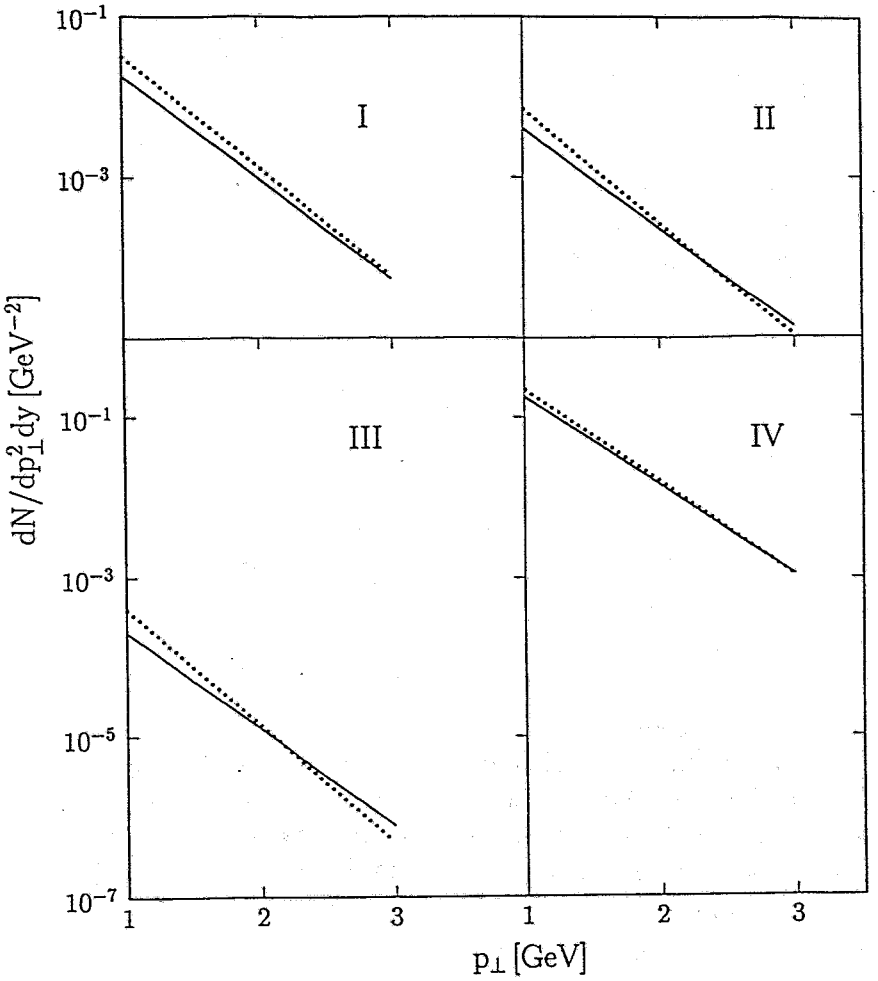

Figure 2: Photon spectra for the initial conditions I - IV described in text. The rate scale factors $\Lambda_{Q,g}$ are 1 (full lines) and 10 (dashed lines).

The space-time integrated rate can be approximated by

$$\frac{dN}{dp_\perp^2\, dy}|_{y=0} = 2\pi \int d\tau\tau dr r d\phi \frac{10}{9}\frac{\alpha\alpha_s}{\pi^4} T^2 \exp\left\{-\frac{\gamma p_\perp}{T}(1+v\cos\phi)\right\}\left(\frac{2\pi T}{\gamma p_\perp}\right)^{1/2} \times \qquad (15)$$

$$\left\{\lambda_Q(\lambda_Q+\lambda_g)\left[\log\left(\frac{3\gamma p_\perp(1+v\cos\phi)}{\pi\alpha_s T}\right) - C_E\right] + \frac{1}{2}\lambda_Q(\lambda_g - 2\lambda_Q)\right\},$$

($E = p_\perp \mathrm{ch}y$) where the integrals have to be performed numerically in conjunction with the solutions of $\gamma(r,\tau) = \sqrt{1+r^2\dot{R}(\tau)^2 R(\tau)^{-2}}$, $v = \sqrt{1-\gamma^{-2}}$, $T(\tau)$ and $\lambda_{Q,g}(\tau)$.

Fig. 2 summarizes our results for the above described four initial conditions and evolution scenarios displayed in Fig. 1 for $R_0 = 7$ fm. One observes at first rather strong variations of the absolute yields according to the suppression discussed. A particular extreme case is III, which relies on the HIJING predictions for the initial conditions [8]. It has to be contrasted to IV (parton cascade [6]). Next one sees that the high-energy photons do not sensitively probe the chemical equilibration velocity. We have chosen drastic variations of $\Lambda_{Q,g} = 1$ or 10 as in Fig. 1. These variations show up in the yield

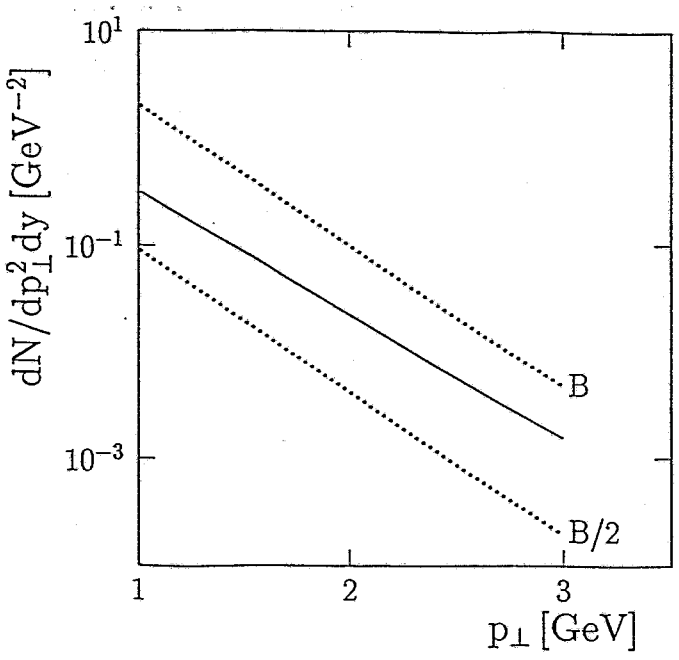

Figure 3: The photon yield from deconfined matter (full line) and hadron matter (dashed lines; the curve labeled by B [B/2] use the standard bag model equation of state with $B^{1/4} = 235$ MeV [equation of state with halved latent heat but the same critical temperature]). The initial temperature is $T_0 = [(g_Q + g_g)/(\lambda_Q^0 g_Q + \lambda_g^0 g_g)]^{1/4} 550$ MeV.

of the medium-energy photons with $p_\perp \sim 1$ GeV: faster equilibration enhances the yield. The harder photons are hardly influenced by variations of the equilibration rates (only for extremely fast equilibration, as anticipated in Ref. [12] the initial temperature drops very fast, which reduces somewhat the high-energy yield). Therefore, the $p_\perp$ spectrum probes the equilibration to some extent, in particular in the softer photon region.

With respect to the results of Ref. [24] one has to investigate also the relation of photons from deconfined matter to photons from hadron matter. According to Ref. [18] and in line with [24] we use the same rates for both matter types. We modify the equation of state by including different values of the bag constant. This has a little effect on the photon yield from deconfined matter down to the critical temperature $T_c = 166$ MeV. (Note that pressure and energy density are changed, but the expansion suffers only minor modification for I, II, IV; for III the thermal pressure is so small that at sufficiently low temperatures the negative vacuum pressure dominates and the system starts to oscillate transversely.) Since the latent heat from the false vacuum decay keeps the system a larger time at T_c, the medium-energy photon yield is somewhat increased (in all cases this is within factor 2 for $p_\perp = 1$ GeV photons). We consider values of $\Lambda_{Q,g}$ large enough, so that $\lambda_Q = \lambda_g = 1$ is reached at T_c. With respect to the results of the parton cascade model [6] this is somewhat extreme for the quark channel, but it has the advantage that the subsequent evolution can be modeled as usually. We find for $B^{1/4} = 235$ MeV in all our examples that, due to the transverse momentum kick from late transverse expansion, the yield from hadron matter is at least a factor 2 larger than the yield from quarks and gluons.

However, the lattice QCD data [10] point to considerably smaller latent heat compared to the bag model. When reducing the latent heat released during the phase transition, but keeping T_c fixed, the photons from deconfined matter dominate significantly in all our examples considered. The reason is that due to reduced latent heat the mixed and hadron phase have a much shorter life time, and a strong transverse flow cannot develop (see Appendix for details). From these studies we conclude that the ratio of photon yield from deconfined matter to the yield from hadron matter depends on the details of the confinement transition. If the latent heat is indeed small and the confinement transition is weakly first-order the photons from parton matter dominate over the thermal hadron yield.

Note that the above considerations rely on a constant initial temperature and varying initial fugacities. One might also assume that the initial energy (or entropy) density of the thermalized state is fixed, and different fugacities cause different initial temperatures. In such a case we find that the photon spectra do not change irrespectively whether fugacities according to I, or II, or IV are considered. Again, for the standard bag model equation of state the hadron matter would shine brighter, while for the reduced latent heat clearly the deconfined matter dominates, see Fig. 3. The rate scaling factors $\Lambda_{Q,g}$ are chosen so that $\lambda_{Q,g} = 1$ is reached at T_c. Variations of $\Lambda_{Q,g}$ which fulfill this condition are not seen on the present scale. With respect to these findings one should argue that the photon spectrum measures the initial energy density, but does not contain separate information on the initial temperature or chemical equilibration.

4 Summary

In summary consider the photon radiation from strongly interacting matter in the framework of a complete scenario including the chemical equilibration of the initial parton matter and its transition through a mixed phase into a hadron gas. Chemical equilibration in a thermalized gluon-enriched plasma is followed within a schematic model of rate equations which includes $gg \rightleftharpoons q\bar{q}$, $gg \rightleftharpoons ggg$ channels and longitudinal and transverse expansion. By variations of the corresponding rates we try to simulate higher order processes. We find that mainly the soft part of the photon spectrum is somewhat sensitive (factor two) to variations of the equilibration rates (when keeping the initial temperature fixed). For fixed initial energy density there is no dependence on the initial phase space saturation, supposed equilibration is fast enough to achieve full local equilibrium at confinement temperature. Provided that deconfined and hadron matter shine equally bright at given temperature, we find that the photons from deconfined matter dominate over hadron matter-created photons in case of a weakly first-order confinement transition, independently of the initial phase space saturation. This provides a good chance to observe thermal photon radiation from early parton matter at energies densities which are presumably achieved in future RHIC experiments.

Acknowledgments: We would like to thank with Y. Asakwa, K. Geiger, J. Kapusta, D. Seibert, E. Shuryak, M. Thoma and G. Zinovjev for stimulating discussions. The work is supported by BMFT under grant 06 DR 107.

References

[1] K. Kajantie, P.V. Landshoff, J. Lindfors: Phys. Rev. Lett. **59** (1987) 2527,
K.J. Eskola, K. Kajantie, J. Lindfors: Nucl. Phys. **B323** (1989) 37

[2] L. van Hove, S. Pokorski: Nucl. Phys. **B86** (1975) 243

[3] E. Shuryak: Phys. Rev. Lett. **68** (1992) 3270
E. Shuryak, L. Xiong: Phys. Rev. Lett. **70** (1993) 2241

[4] X.N. Wang, M. Gyulassy: Phys. Rev. **D44** (1991) 3501

[5] K. Geiger, B. Müller: Nucl. Phys. **B369** (1992) 600
K. Geiger: Phys. Rev. **D46** (1992) 4965, 4986, **D47** (1993) 133
K. Geiger, J.I. Kapusta: Phys. Rev. Lett **70** (1993) 1920

[6] K. Geiger, J. Kapusta: Phys. Rev. **D47** (1993) 4905

[7] I. Kawrakow, J. Ranft: preprint UL-HEP-92-08

[8] T.S. Biro, E. van Doorn, B. Müller, M.H. Thoma, X.N. Wang: Duke-TH-93-46, Phys. Rev. **C** in print

[9] H. Satz: Nucl. Phys. **A544** (1992) 169c

[10] J. Engels, J. Finberg, F. Karsch, M. Weber: Phys. Lett. **B252** (1990) 625
F. Karsch: in Particle Production in Highly Excited Matter, (Eds.) H.H. Gutbrod, J. Rafelski, Plenum Press New York - London 1993, NATO ASI series **303B**, p. 649

[11] P.V. Ruuskanen: Nucl. Phys. **A544** (1992) 371c

[12] L. Xiong, E. Shuryak, preprint SUNY-NTG-93-24

[13] R. Schmidt, J. Schukraft: preprint GSI-92-19
K.H. Kampert al. (WA80 collaboration): preprint IKP-MS-93/0302,
talk given at the Spring Meeting of the German Physical Society, Mainz, 26 March 1993

[14] M.H. Thoma: Proc. Inst. Workshop, Hirschegg XXI 1993, (Ed.) H. Feldmeier
H. Heiselberg, G. Baym, C.J. Pethick, J. Popp: Nucl. Phys. **A544** (1992) 569c

[15] P. Lichard, M. Prakash, SUNY-NTG-92-42

[16] B. Kämpfer, O.P. Pavlenko, preprint FZR-93-09, FZR-93-16, Proc. of Quark Matter '93, to be published in Nucl. Phys. **A**

[17] V.V. Klimov: Yad. Fiz. **33** (1981) 1734 [Sov. J. Nucl. Phys. **33** (1981) 934],
H.E. Weldon: Phys. Rev. **D26** (1982) 2789

[18] J. Kapusta, P. Lichard, D. Seibert: Phys. Rev. **D44** (1991) 2774

[19] R. Baier, H. Nakkagawa, A. Niégawa,, K. Redlich: Z. Phys. **C53** (1993) 433

[20] A. Dumitru, D. Rischke, H. Stöcker, W. Greiner, UFTP 308/1992

[21] J. Cleymans, V.V. Goloviznin, K. Redlich: Phys. Rev. **D47** (1993) 989

[22] E. Braaten , R.D. Pisarski: Phys. Rev. Lett. **64** (1990) 1338, Nucl. Phys. **B337** (1990) 569

[23] H. Satz: Nucl. Phys. **A544** (1992) 371c

[24] J. Alam, D.K. Srivastava, B. Sinha, D.N. Basu: Phys. Rev. **D48** (1993) 1117

[25] B. Kämpfer, M.I. Gorenstein, O.P. Pavlenko: Z. Phys. **C45** (1990) 491

[26] T. Biro, H.W. Barz, B. Lukács, J. Zimanyi: Phys. Rev. **C27** (1983) 2695
H.W. Barz, B. Friman, J. Knoll, H. Schulz: Nucl. Phys. **A545** (1992) 397

[27] E. Schnedermann, U. Heinz: preprint TPR-92-42

[28] H.W. Barz: private communication, to be published

[29] J. Kapusta, L. McLerran, D.K. Srivastata: Phys. Lett. **B283** (1992) 145

A Global hydrodynamics for transverse expansion

A.1 Basic equations

Rate equations are suitably solved in comoving fluid cells. This has been done, e.g. in Ref. [25]. Here we develop a simpler scheme which relies on transverse spatial averages of intensive densities. In doing so the partial differential equations of relativistic hydrodynamics are converted into ordinary differential equations. In case of spherical symmetry such an approach is used in Refs. [26]. A recent paper [27] employs a similar approach to cylinder symmetry with prescribed trial functions for thermodynamic and kinematic quantities. Our approach is for a transverse expansion superimposed on longitudinal boost-invariant scaling hydrodynamics.

The hydrodynamical equations read $\partial_\mu T^{\nu\mu} = 0$, where the energy-momentum tensor $T^{\mu\nu} = \int d^3pE^{-1}p^\mu p^\nu f$ is decomposed for the supposed case of thermal equilibrium as $T^{\mu\nu} = (e+p)u^\mu u^\nu + pg^{\mu\nu}$ with e and p as energy density and pressure, and $g^{\mu\nu}$ as Minkowski metric. The boost-invariant four velocity reads in case of axisymmetry in Cartesian coordinates

$$u^\mu = \gamma(\mathrm{ch}\eta, v\cos\phi, v\sin\phi, \mathrm{sh}\eta), \quad \gamma = (1-v^2)^{1/2}, \tag{A.1}$$

where v is the transverse velocity, and η stands for the longitudinal rapidity. The velocity-projected equation $u_\mu\partial_\nu T^{\mu\nu} = 0$ and the time-like component of the equations of motion $\partial_\mu T^{0\mu} = 0$ represent two independent equations,

$$\partial_\mu(eu^\mu) + p\partial_\mu u^\mu = 0, \tag{A.2}$$

$$\partial_t T^{00} + \partial_z(T^{00}+p)\tfrac{z}{t} - \partial_x(T^{00}+p)\tfrac{\tau}{t}v\cos\phi - \partial_y(T^{00}+p)\tfrac{\tau}{t}v\sin\phi = 0. \tag{A.3}$$

In the coordinate system $\tau = \sqrt{t^2-z^2}$, $\eta = \frac{1}{2}\log\frac{t+z}{t-z}$, $r = \sqrt{x^2+z^2}$ these equations become on the central slice $z = 0$

$$\partial_\tau(e\gamma) + p\partial_\tau\gamma + (e+p)\frac{\gamma}{\tau} + \frac{1}{r}\partial_\tau(e\gamma vr) + \frac{p}{r}\partial_\tau(\gamma vr) = 0, \tag{A.4}$$

$$\partial_\tau(e\gamma^2) + \partial_\tau(p\gamma^2v^2) + (e+p)\frac{\gamma^2}{\tau} + \frac{1}{r}\partial_\tau([e+p]\gamma^2vr) = 0. \tag{A.5}$$

By performing a radial integration $\int dr\, r$(A.4, A.5) we get rid of the gradients $\partial_\tau(\ldots)$ via Gauss's law. The essential point is the factorization ansatz of intensive densities and kinematic quantities, e.g., $\int dr\, re\gamma = \bar{e}\int dr\, r\gamma \equiv \bar{e} < \gamma >$, where $\bar{e}$ stands for the transverse average. This ansatz is fulfilled for $e = e(\tau)$, i.e., a homogeneous transverse distribution. Hence we get

$$\partial_\tau(e < \gamma >) + p\partial_\tau < \gamma > +(e+p)\frac{< \gamma >}{\tau} = 0, \tag{A.6}$$

$$\partial_\tau(e < \gamma >^2) + \partial_\tau(p < \gamma^2 v^2 > +(e+p)\frac{< \gamma^2 >}{\tau} = 0, \tag{A.7}$$

where we omit the bar for indicating the averages. Eqs. (A.6, A.7) are to be read as ordinary differential equations, because there is only a remaining time dependence.

In case of validity of the Gibbs relation $e + p = Ts$ and $s = \partial p/\partial T$ (we consider charge-symmetric media with $\mu = 0$) eq. (A.6) gives $s < \gamma > \tau = const$, which can be used for checking the numerical accuracy in solving eqs. (A.6, A.7). In a two-phase mixture the thermodynamic relations need to be modified, cf. e.g. [25].

To proceed one must specify a trial velocity profile. We employ

$$v\gamma = \frac{\dot{R}}{R}r \tag{A.8}$$

with $R(\tau)$ as transverse radius. Such a linear profile is supported by extensive cascade-like calculations for the transverse expansion of a finite particle system with medium-corrected cross sections [28]. With

$$< \gamma > = \frac{R^2}{3\dot{R}^2}([1+\dot{R}^2]^{3/2} - 1), \tag{A.9}$$

$$< \gamma^2 > = \frac{1}{2}R^2(1 + \frac{1}{2}\dot{R}^2), \tag{A.10}$$

$$< \gamma^2 v^2 > = \frac{1}{4}R^2\dot{R}^2, \tag{A.11}$$

the equations to be solved read

$$\dot{e}(1 + 2[1 + \frac{1}{2}\dot{R}^2]\mathcal{K}) + \dot{p}\dot{R}^2\mathcal{K} + (e+p)(2\frac{\dot{R}}{R} + \frac{1}{\tau} + 2\mathcal{K}[2\frac{e}{e+p}\frac{\dot{R}}{R} + \frac{\dot{R}^3}{R} + \frac{1}{\tau}\{1 + \frac{1}{2}\dot{R}^2\}]\mathcal{K}) = 0, \tag{A.12}$$

$$\ddot{R}(1+2\mathcal{K}) - \frac{2}{R}\frac{p}{e+p} + \frac{(\dot{e}+\dot{p})\dot{R}}{2(e+p)} + \frac{\dot{R}}{2\tau} + \frac{\dot{R}^2}{r} = 0, \tag{A.13}$$

$$\mathcal{K} = 1 + \frac{1}{\dot{R}^2}\left(1 - \frac{3}{2}\frac{\dot{R}^2(1+\dot{R}^2)^{1/2}}{(1+\dot{R}^2)^{3/2} - 1}\right).$$

The eq. (A.13) shows that the transverse expansion is driven essentially by the pressure (the other terms are the usual relativistic corrections). Care is to be taken with the initial stage where $\dot{R}$ may vanish. The equations are solved together with the rate equations by standard methods. The temperature is calculated from the energy density e. For $\dot{p}$ the equation of state is to be used. These equations replace the longitudinal expansion eqs. (26) in Ref. [8] or (33) in Ref. [12].

For completeness we display also the corresponding evolution equation of the particle density. From $\partial_\mu(nu^\mu) = 0$ follows

$$\dot{n} + \frac{n}{\tau} + n\frac{\dot{<\gamma>}}{<\gamma>} = 0, \tag{A.14}$$

which shows how the transverse degree of freedom affects the particle dilution.

A.2 Influence of transverse expansion on photon spectra

To check the credibility of the global hydrodynamics we recalculate the photon yield as in Ref. [24]. The chosen initial conditions are $\tau_0 = 0.13$ fm/c, $T_0 = 532$ MeV as in Refs. [24, 29] for RHIC conditions, and full phase space saturation is assumed. As [24] we find that the photon yield from the hadron phase exceeds that from the deconfined phase due to the transverse momentum kick in the very late expansion stage, see Fig. A.1. This lends credibility to our global hydrodynamical scheme, where no steep gradients drive the transverse expansion. This result is found for a bag model equation of state with bag constant $B^{1/4} = 235$ MeV, and degeneracies 40 (3) for the deconfined (confined) phase.

Since the strong contribution of hadron matter-created photons come in the hydrodynamical model at very late time (see Fig. A.1), one might be suspicious, whether the large latent heat in the used bag model equation of state is responsible for the main result in Ref. [24]. Indeed, when using a bag constant $\frac{1}{2}B$ instead of B, and rescaling the degeneracy in the hadron phase so that the critical temperature stays constant, the yield from hadron matter strongly reduces and falls below the yield from the quark-gluon plasma, see Fig. A.1. Variations of the bag constant have only a small effect on the yield from quark-gluon plasma (not seen on this scale). Marginal deviations to Fig. 17 in Ref. [24] arise from slightly different photon rate equation, and different α_s, and the use of global hydrodynamics. Due to the halved latent heat the system freezes out (we use as Ref. [24] $T_{freeze-out} = 120$ MeV) at much shorter time (7 instead 18 fm/c for RHIC conditions) smaller radius (11 instead of 20 fm). In reducing B, while keeping T_c fixed, not only the latent heat is reduced but the pressure in the deconfined phase increases and the energy density decreases. The net effect of several competing effects however is a strongly reduced life time of both the mixed and the hadron stages. As consequence, the transverse flow has not time enough to develop. Since recent lattice QCD calculations [10] point to much smaller latent heat than previous bag models, one should expect that the anticipated effect of the very strong transverse photon kick [24] is an upper bound which becomes smaller for more realistic equations of state.

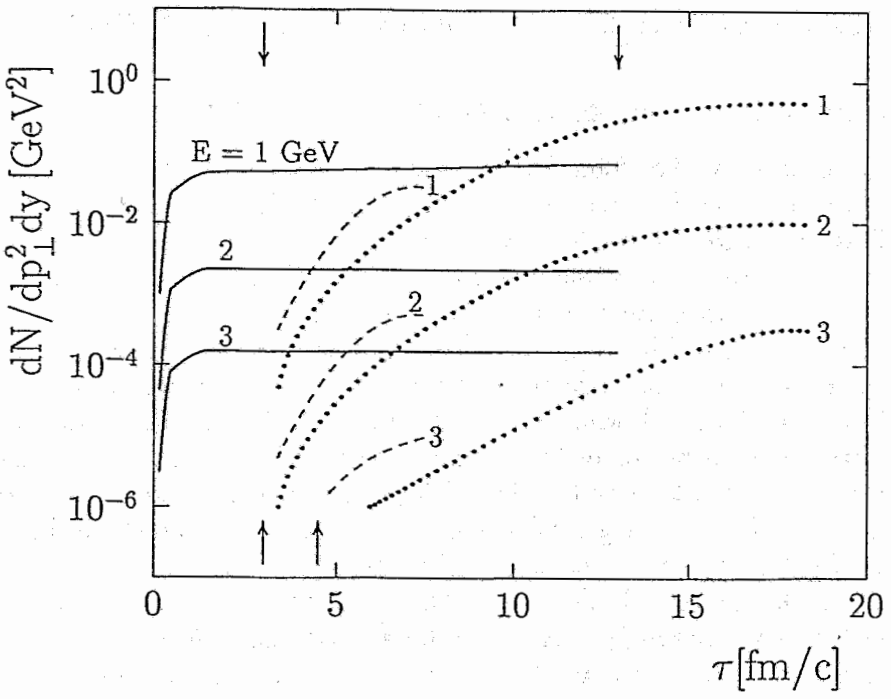

Figure A.1: Photon yields for several photon energies $E = p_\perp \mathrm{ch}y$ for RHIC conditions (as described in text) for QGP (full lines) and hadron matter (dashed lines with $B^{1/4} = 235$ MeV, and dotted lines for halved latent heat and fixed T_c). The upper (lower) pair of arrows indicates the beginning and end of the mixed phase for the standard bag model equation of state (equation of state with halved latent heat).